Chemistry & Biology, Vol. 12, 201–206, February, 2005, ©2005 Elsevier Ltd All rights reserved. DOI 10.1016/j.chembiol.2004.11.019

Coevolution of Protein and RNA Structures within a Highly Conserved Ribosomal Domain

Mark S. Dunstan,[1] Debraj GuhaThakurta,[2,3] David. E. Draper,[2] and Graeme L. Conn[1,*]
[1]Faculty of Life Sciences
University of Manchester
Jackson's Mill
P.O. Box 88
Manchester, M60 1QD
United Kingdom
[2]Department of Chemistry
The Johns Hopkins University
3400 North Charles Street
Baltimore, Maryland 21218

Summary

The X-ray crystal structure of a ribosomal L11-rRNA complex with chloroplast-like mutations in both protein and rRNA is presented. The global structure is almost identical to that of the wild-type (bacterial) complex, with only a small movement of the protein α helix away from the surface of the RNA required to accommodate the altered protein residue. In contrast, the specific hydrogen bonding pattern of the mutated residues is substantially different, and now includes a direct interaction between the protein side chain and an RNA base edge and a water-mediated contact. Comparison of the two structures allows the observations of sequence variation and relative affinities of wild-type and mutant complexes to be clearly rationalized, but reinforces the concept that there is no single simple code for protein-RNA recognition.

Introduction

Ribosomal protein L11 and its RNA binding domain (nucleotides 1051–1108 of the large subunit rRNA, *E. coli* numbering; see Figure 1) are among the most highly conserved components of the ribosome [1]. Nonetheless, a limited number of specific, coordinated primary sequence variations have occurred within this domain that have provided useful structural and functional insight. For example, a comparative analysis of rRNA sequences led to the initial identification of a base triple interaction in the rRNA tertiary fold [2] that was subsequently confirmed by X-ray crystallographic structures of the domain [3, 4]. A similar approach was also applied to rRNA and protein sequences: L11 residue 69, although almost universally conserved as serine (Ser) throughout the three domains (eubacteria, archaebacteria, and eukaryotes), was found to vary to asparagine (Asn) in all known chloroplast sequences and one closely related cyanobacteria, *Synechocystis* [5]; this was invariably accompanied by a coordinated change of the rRNA base pair GC1062-1076 to either a UA pair or UC mismatch [6]. L11 shares a protein fold with the homeodomain class of DNA binding proteins where the equivalent position (51) is always Asn, and is a critical component of the protein-DNA interaction [7]. Mutation of bacterial (*Bacillus stearothermophilus*) L11 to the chloroplast-like (ch-like) Asn69 substantially reduced binding to wild-type rRNA, while Ser69 protein bound RNAs with G-C and U-A base pairs at 1062/1076 with roughly equal affinity [6]. Mutation of position 69 to alanine reduced binding to both RNAs [6, 7].

Based on these observations, it was proposed that the covariation of L11 position 69 and rRNA base pair 1062/1076 represented an example of "direct compensation," i.e., the substitution of a base-amino acid interaction with an isosteric set of hydrogen bonds to yield a complex of equivalent stability. (In contrast to an alternative situation where maintenance of complementary surfaces requires an extensive set of changes to accommodate the mutation of an amino acid or RNA nucleotide.) Here, we present the X-ray crystal structure of a ch-like rRNA-L11 complex that reveals an extensively altered set of hydrogen bonding interactions made by the mutated residues; however, only very minimal alteration to the global folds of either protein or RNA are required to accommodate the changes. Comparison of the wild-type and ch-like structures allows the covariations and relative binding affinities for L11(C76) to be readily rationalized, and illustrates an example of a natural coevolution of RNA and protein structures required to maintain an important element of protein-RNA recognition in a functional complex.

Results and Discussion

Ch-like rRNA Tertiary Structure Stability and L11(C76) Binding Affinity

Unfolding of the tertiary structure in the 58 nucleotide rRNA domain is characterized by strong hyperchromicity at 260 nm relative to 280 nm allowing it to be readily identified in melting profiles determined at these wavelengths [8]. The melting profiles of wild-type and ch-like RNAs are shown in Figure 2. Both rRNA domain tertiary structures are extremely stable and unfold with high apparent T_ms (see Table 1). The ch-like GC1062-1076UA mutation destabilizes the RNA tertiary structure such that it cannot be detected in the absence of compensatory stabilizing mutations (as discussed below, this appears to be due, at least in part, to a significant alteration in base stacking around the 1062-1076 base pair). With additional mutations GC1089/1090UA, the ch-like RNA (chRNA3 [6]; see Experimental Procedures) has a tertiary T_m of 46°C, compared to 59°C for the stabilizing mutation made in the wild-type context. The mutation U1061A has a similar stabilizing effect in the wild-type context (T_m of 58°C; Figure 2). For this study, both the AA1089/1090GU and U1061A mutations were incorporated into the ch-like RNA; the effects are clearly additive as the apparent T_m increases further from 46°C (for AA1089/90GU alone) to 56°C with mutations at both sites.

*Correspondence: graeme.l.conn@manchester.ac.uk
[3]Present address: Rosetta Inpharmatics, Inc. (Merck & Co.), Kirkland, Washington.

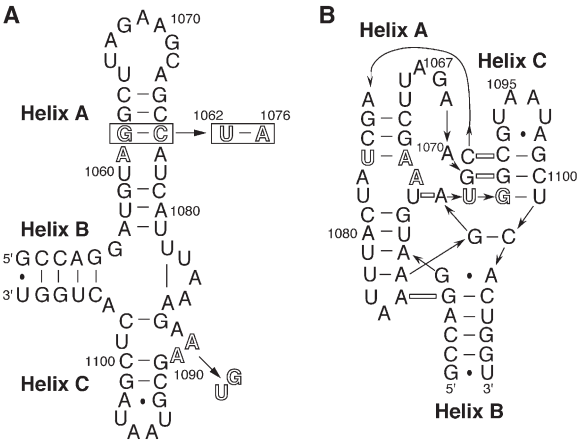

Figure 1. Secondary and Tertiary Structures of the 58 Nucleotide L11 Binding Domain rRNA

(A) rRNA secondary structure showing the bases mutated in the ch-like RNA sequence in outline font. The base pair involved in covariation with L11 amino acid 69 (1062-1076) is boxed; other mutations, AA1089/1090GU and U1061A, were introduced to stabilize the RNA tertiary structure. The latter mutation was present in both RNAs used in this study (see Experimental Procedures).

(B) rRNA secondary structure redrawn according to the RNA fold determined in the X-ray crystal structure, with tertiary RNA-RNA contacts shown as open bars.

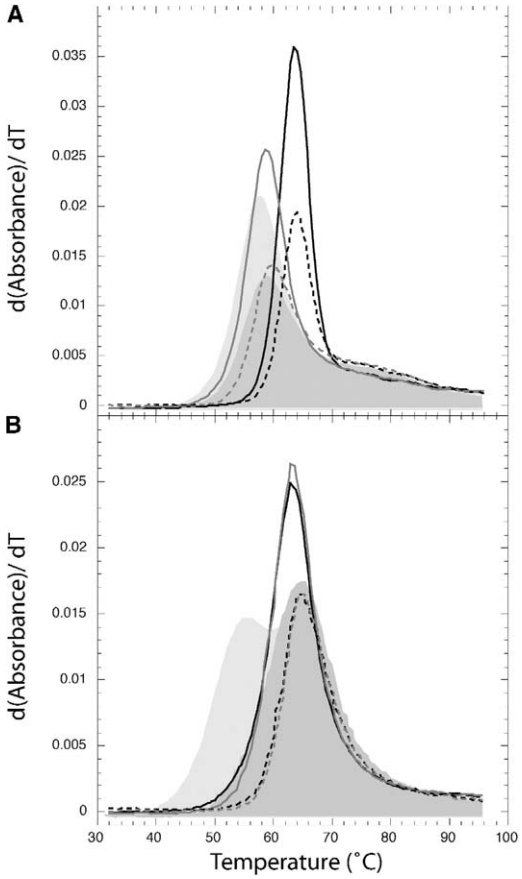

Figure 2. UV Melting Profiles of Stabilized Wild-Type and Ch-like RNAs in the Absence and Presence of Each L11 Variant

(A) Melting profiles of stabilized wild-type RNA in the absence (260 nm and 280 nm profiles shown as light gray and dark gray shadows, respectively) and presence of wild-type L11(C76)Ser69 (black) and ch-like mutant L11(C76)Asn69 (gray); for melts with proteins, 260 nm profiles are shown as solid lines, and 280 nm profiles as dashed lines.

(B) Melting profiles for ch-like RNA and wild-type (black) and mutant Asn69 (gray) L11(C76) depicted as in (A).

L11(C76) is known to increase the stability of the RNA tertiary structure and each protein-RNA combination was tested in melting experiments (Figure 2). Asn69 L11(C76) stabilizes the ch-like RNA tertiary structure by ~9°, but has little effect on the apparent T_m for wild-type RNA tertiary unfolding; in contrast, the wild-type Ser69 protein stabilizes both rRNAs equally. The effects of the L11(C76) variants on each rRNA tertiary structure stability thus correlate well with relative binding affinities determined in nitrocellulose filter binding affinity assays (shown in Table 1) [6, 7]. The ch-like RNA used for the earlier study bound L11(C76)Ser69 and Asn69 with roughly equal affinity (Table 1), and with a value of the same order for the interaction of the authentic *E. coli* RNA and L11(C76)Ser69 (not shown). In contrast, the wild-type RNA (actually a variant containing mutations required to give detectable tertiary folding for ch-like RNAs; see Experimental Procedures for details) showed a 20-fold discrimination between the proteins. Neither RNA bound L11(C76)Ala69 with high affinity (Table 1).

Crystallization and Model Building

The original plasmid used for RNA in vitro transcription produced a ch-like RNA with an overhanging 5′-G nucleotide in addition to the 58 nucleotides of the rRNA sequence shown in Figure 1 (this was incorporated in earlier studies to give a stronger T7 RNAP promoter and thus increase RNA yields). This RNA, complexed with the L11(C76)Asn69 protein, produced large but very thin plate-like crystals with the crystallization conditions previously used for the wild-type complex [3]. Removal of the 5′-G nucleotide to give a ch-like RNA with a blunt-ended helix B (Figure 1) produced large crystals of the ch-like complex from conditions very similar to those used for the wild-type complex. This clearly illustrates the effect that even very small modifications in RNA sequence/structure can have on crystallizability or the quality of crystals obtained. In this case, helix B from two RNA molecules in adjacent asymmetric units make a crystal lattice contact via end-to-end stacking interactions (i.e., G1051 on U1108′ and G1051′ on U1108), which is presumably disrupted by the presence of an additional nucleotide on each RNA 5′-end.

The mutated RNA and protein residues, and numerous ions, waters and glycerol molecules were clearly visible in the $2F_o - F_c$ and $F_o - F_c$ maps produced by molecular replacement (see Experimental Procedures). The majority of these ions and waters are in (or close to) equivalent sites observed in the original structure. Glycerol molecules, distinguished from ions and ordered waters by the shape and extended nature of the density, were not observed in the previous structure. Presumably the addition of glycerol to the crystallization solution, rather than addition immediately prior to freezing the crystal, has allowed these molecules to lo-

Table 1. Affinities for Wild-Type and Mutant L11(C76)-rRNA Complexes

	Relative Binding Affinities[a]		Apparent RNA Tertiary T_m (°C)[b]	
L11(C76) protein	Wild-Type RNA	Ch-like RNA	Wild-Type RNA	Ch-like RNA
None	—	—	58	55
S69	*1.00*	0.23	64	64
N69	0.05	0.26	59	64
A69	0.09	0.03	ND	ND

[a] Relative binding constants normalized to the complex with wild-type RNA base pair GC1062-1076 and L11(C76)Ser69 (italics), measured by nitrocellulose filter binding assays [6].
[b] Apparent RNA tertiary structure T_ms in the absence and presence of each protein are taken from the UV melting data shown in Figure 2 (ND, not determined). Details of the RNA sequences used in each column are given in the Experimental Procedures.

cate favorable sites with much higher occupancy. The quality of the final solution was demonstrated by the generation of omit maps, excluding RNA residues UA1062-1076 and amino acids 69; these omit maps were used in the preparation of Figure 3A.

Structure of the Ch-like RNA:L11-C76(Asn69) Complex

The global structure of the ch-like RNA-L11(C76) Asn69 complex was, as expected, extremely similar to the wild-type complex with rmsds for backbone alignment of wild-type/ mutant RNAs and proteins of 0.38 and 0.31 Å, respectively. There was however, a small change in the L11-C76 main chain conformation around the site of the Ser69Asn mutation, that moves the C-terminal end of the α helix further from the RNA surface (Figure 3A). Presumably this is required partly to accommodate the larger Asn69 side chain, though the alteration of RNA base 1062 from a purine to a pyrimidine is also likely a significant factor in preventing steric clashes. Despite the minimal modification to the overall structure of the rRNA-L11(C76) complex, the set of hydrogen bonding interactions involved in protein-RNA recognition is dramatically altered. The Asn69 side chain is reorientated so that it points directly toward the UA1062-1076 base pair edge in the RNA minor groove (Figure 3B), where a hydrogen bonding interaction is made between the Asn69 NH_2 and U1062 carbonyl (Figure 3C). A further hydrogen bonding interaction is made between the Asn69 NH_2 group and N3 of the adjacent, universally conserved A1077 (which, in turn, is involved in tertiary interactions with the backbone at A1088 and A1089 in both wild-type and mutant structures). The carbonyl group of the Asn69 side chain makes a third hydrogen bonding interaction with ribose 2′-OH of A1077. The backbone carbonyl of residue 69, which for wild-type Ser69 contacts the RNA base edge (Figure 3D), no longer hydrogen bonds to the RNA directly but instead lies beneath the G1063 ribose and appears to contact a partially ordered water molecule. In the Ser69 structure, the side chain adopts a gauche(–) conformation and makes two hydrogen bonding interactions: one to the backbone carbonyl group of Thr66 and the other to the 2′-OH of U1062 (Figure 3D). In the ch-like mutant structure, this set of interactions appears to be replaced by solvent mediated hydrogen bonding as the same partially ordered water is seen adjacent to these residues (Figure 3C).

The X-ray crystal structure of the ch-like complex allows contrasting observations on the nature of L11-rRNA recognition to be readily rationalized. Comparing the observed hydrogen bonding patterns in the wild-

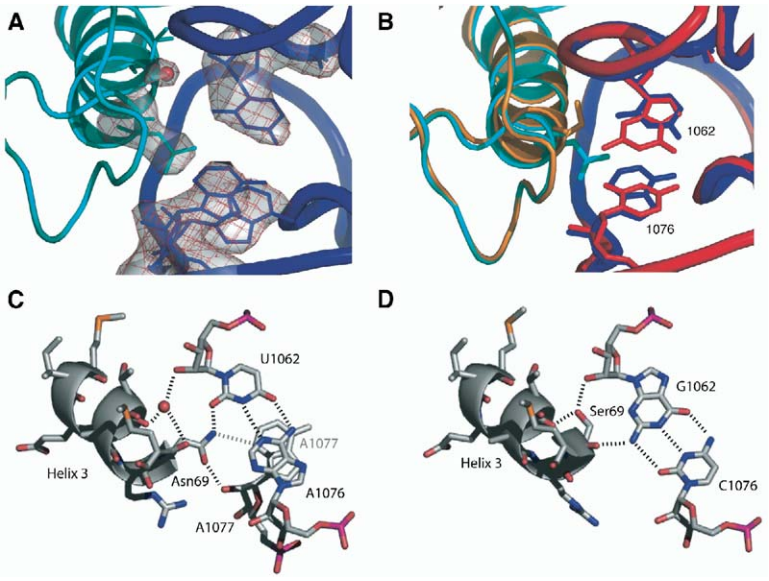

Figure 3. Interactions in the Ch-like rRNA-L11(C76) Complex

(A) The structure of the ch-like RNA base pair UA(1062-1076) and L11(C76)Asn69. $2F_o - F_c$ electron density (contoured at 1 σ) shown around the RNA nucleotides and L11 amino acid was generated with these residues omitted.

(B) Alignment of the protein and RNA backbones, with base pair 1062-1076 and L11 residue 69 shown for both wild-type and ch-like structures. Wild-type L11(C76)Ser69 protein/ rRNA are shown in orange/red, and mutant L11/rRNA in cyan/blue.

(C and D) Comparison of the observed hydrogen bond patterns for the ch-like and wild-type L11-rRNA complexes, respectively. In the ch-like mutant complex, the Asn69 side chain is oriented so that it makes a direct interaction with U1062 in the minor groove. All images were generated in PyMOL [17].

Table 2. X-Ray Crystallographic Data Collection, Refinement, and Model Statistics

Space group	$P4_32_12$
Unit cell a, b, c (Å)	150.2, 150.2, 63.0
Resolution range (Å)	18.0–2.8 (2.9–2.8)
Reflections	
Total	85,706
Unique	17,767
Average redundancy	4.8 (4.9)
Completeness (%)	97.5 (98.1)
R_{merge}	0.061 (0.445)
I/sigI	18.0 (5.1)
R_{work} (%)	22.7
R_{free} (%)	25.5
Rmsd bonds (Å)	0.0063
Rmsd angles (°)	1.119

Values in parentheses are for the highest resolution shell.

type and mutant complexes (Figures 3C and 3D) reveals a substantially altered set of interactions between the different sets of residues. With Ser69, a favorable set of hydrogen bonding interactions is obtained by positioning the amino acid side chain so that it points away from the base edges and contacts backbone groups of the RNA and protein (Figure 3D); as these interactions are independent of the RNA base identity, L11(C76)Ser69 binds both wild-type and ch-like RNAs with approximately equal affinities, and stabilizes the rRNA tertiary structure to the same extent. In contrast, the Asn69 side chain does not make these nonsequence-specific interactions, but instead contacts the 1062 base edge, directly probing the identity of the base at this position. This direct recognition of the base carbonyl group explains the preference of L11(C76)Asn69 for ch-like rRNA over wild-type where the smaller pyrimidine base with a carbonyl group is replaced by a larger purine with NH_2. In the ch-like rRNA sequence, cytosine is actually more commonly found at position 1062; as both uridine and cytosine present a carbonyl group in the minor groove, in terms of recognition by Asn69, these are indistinguishable. The sequence covariations, and modest structural modifications required to accommodate them, suggest that L11 and the rRNA domain have coevolved to maintain a key interaction involved in protein-RNA recognition. Clearly, the mutation of RNA base pair and single amino acid does not simply involve the exchange of one set of isosteric residues for another but rather a major alteration of the hydrogen bonding pattern at the protein-RNA interface. This parallels observations in protein-DNA recognition, for example in the binding of several variants of the zinc finger motif to different DNA recognition sequences. There, although related substitutions of side chain-base interactions were identified, no simple correspondence between protein residue and base substitutions could be identified and the situation was often complicated by the involvement of water molecules [9]. The structure of the ch-like L11-rRNA complex may likewise substitute water for some protein-RNA contacts, and reinforces the idea there is no simple code for protein-RNA recognition.

The ch-like GC1062-1076UA mutation is destabilizing and results in the loss of correct RNA tertiary folding in the absence of other stabilizing mutations. A possible reason for this is apparent from the structure of the ch-like complex. Base 1062 is positioned adjacent to G1063 and A1077 in an extended stack of bases, distorted from a standard A-form helical geometry by the RNA tertiary structure. From visual inspection of the two structures, G1062 appears to form a better stacking arrangement than the ch-like U1062, which would thus favor a more stable RNA tertiary fold. We note, however, that the complete explanation may not be this simple as the ch-like mutations could have other subtle influences on RNA tertiary structure stability; for example, the major groove side of this base pair is near Mg^{2+} in a site of high electrostatic potential [10] important for correct tertiary folding.

Significance

Protein-RNA recognition is dependent upon mutual surface complementarity including geometric constraints and the potential for hydrogen bonding interactions. The X-ray crystal structure of an L11-rRNA ribosomal domain containing a set of chloroplast-like mutations showed that such changes could be accommodated with minimal modification of the global structure of the complex. However, detailed examination revealed an extensively altered set of hydrogen bonding interactions for the mutated residues, indicating that there is unlikely to exist one simple code for protein-RNA recognition. Comparison of the wild-type and mutant complexes allows a number of previous observations to be rationalized. First, the destabilizing effect of the ch-like base pair mutation on the RNA tertiary structure can be explained, at least in part, by a detrimental alteration in base stacking (though this can be compensated for by stabilizing other parts of the tertiary structure). Second, the altered hydrogen bonding pattern fully explains the observed natural sequence covariations, and the measured relative binding affinities for wild-type and mutant complexes. This structure thus clearly illustrates an example of natural coevolution of RNA and protein structures to maintain an important recognition contact in a functional complex. We have recently found that mutations destabilizing the L11-rRNA interaction by >5 kcal/mol cause detectable effects in vivo, while destabilization of >8 kcal/mol is lethal (C. Maeder, G.L.C., and D.E.D., unpublished data). Both findings support our earlier suggestion that stabilization of the correct rRNA tertiary fold may be the major role of L11 [3]. We would propose that the maintenance of a high affinity interaction between L11 and its 58 nucleotide rRNA binding domain is essential for efficient ribosome function (e.g., through an influence on ribosome factor binding or function) and that this has provided the driving force for the observed coevolution of rRNA and protein.

Experimental Procedures

RNA Sequences, RNA In Vitro Transcription, and Protein Expression

Two versions of the 58 nucleotide RNA sequence were used in this study. The first, a stabilized version of the *E. coli* wild-type (with

mutation U1061A), was that used in our original X-ray structure determination [3]. The second was constructed as described below and contained the ch-like mutations GC1062-1076UA, and stabilizing mutations U1061A and AA1089/1090GU. For simplicity, these two RNAs are referred to as "wild-type" and "ch-like" (i.e., with respect to the relevant 1062-1076 base pair). Several other RNA sequence variants, including the authentic *E. coli* wild-type, a stabilized AA1089/1090GU mutant, and several ch-like RNAs, were compared in a previous study [6]. Two of these, AA1089/1090GU RNA and one ch-like RNA ("chRNA3"), are used for comparison with the data presented here (see Table 1). The ch-like GC1062-1076UA mutation is very destabilizing and chRNA3 thus contained second-site mutations (AA1089/1090GU; but not U1061A) to stabilize the RNA tertiary structure. Like the U1061A stabilized variant used here, the AA1089/1090GU RNA is wild-type with respect to the 1062-1076 base pair. Both these RNAs bind L11(C76)Ser69 (i.e., wild-type protein) with equal affinity, and approximately 3-fold higher than the authentic *E. coli* sequence [2, 6].

A pUC18 derivative containing DNA corresponding to chRNA3 [6] was used as a starting point for generating the ch-like RNA used in this study. An additional, overhanging 5′-G nucleotide was removed and the U1061A mutation made by QuikChange site-directed mutagenesis (Stratagene) so that the ch-like RNA produced was exactly the sequence shown in Figure 1. RNAs were transcribed by run-off transcription from RsaI linearized plasmid using T7 RNAP (expressed from plasmid pT7-911 and purified by Ni^{2+} affinity chromatography [11]) and purified by denaturing polyacrylamide gel electrophoresis using 12% acrylamide gels. RNA containing bands were identified by UV shadowing and excised, and the RNA recovered by electroelution using a BioTrap device (Schleicher & Schuell) followed by ethanol precipitation.

pET11a-based plasmids for overexpressing L11-C76 (the RNA binding C-terminal 75 residues of ribosomal protein L11 from *Bacillus stearothermophilus*) and the Asn69 variant have previously been described [6, 7]. These were used to transform *E. coli* BL21 cells, and each protein expressed and purified essentially as described [7]. Briefly, purification was achieved in two chromatographic steps: first by size exclusion on Sephacryl S-200 resin, and second, by cation exchange using a 1 ml Hitrap SP FF on an ÄKTA-purifier 100 FPLC. The concentrations of L11-C76 and S69N solutions were calculated from absorbance measurements at 230 nm using an extinction coefficient of 24.8×10^3 $M^{-1}cm^{-1}$, calculated on the basis of quantitative amino acid analysis [7].

UV Melting Analysis of Wild-Type and Mutant 58 Nucleotide RNAs

Samples contained ~20–25 μg RNA in a solution containing 10 mM MOPS buffer (pH 7.0), 175 mM KCl, and 5 mM $MgCl_2$. UV melting curves were measured on a Varian Cary 400 UV/Vis spectrophotometer, equipped with a 6 cell multichanger and temperature probe, running in dual beam mode. Up to five RNA melting curves were collected in a single run; the sixth position was used for the temperature probe inserted into a sample of buffer. Data points were collected at 0.5°C intervals between 30ºC and 98°C with a heating rate of 0.5°C/min. The "melting profiles" presented here are the first derivatives of the raw melting curves averaged over a 5°C window and normalized to the absorbance at 35°C with the program OD Deriv [12] (http://ded.chm.jhu.edu/~draper/index.html).

Crystallization, X-Ray Data Collection, and Structure Determination

Equimolar amounts of L11-C76 and RNA were mixed to yield a 1:1 protein-RNA complex at a concentration of 0.35 mM. To aid the correct folding of the RNA, the sample was annealed by heating to 65°C for 10 min and slow cooling to room temperature. Crystals were grown at 37°C by hanging drop vapor diffusion in 15% glycerol, 50 mM sodium cacodylate buffer (pH 6.5), 15% PEG 600, 80 mM $Mg(OAc)_2$, 100 mM KCl, and 0.2 mM $Co(NH_3)_6Cl_3$. Suitable crystals grew in 1–2 days and were flash-frozen in liquid nitrogen directly from the crystallization drops. Data were collected from a single crystal under cryogenic conditions on beamline 9.6 at the Synchrotron Radiation Source (SRS, Daresbury Laboratories) over a 61° range, and with an oscillation angle of 0.5°. The data were integrated and scaled using D*Trek from the CrystalClear data processing software package (Rigaku/MSC, Inc., The Woodlands, TX).

The crystal structure of L11-C76 bound to a variant of the 58 nucleotide *E. coli* 23S rRNA sequence 1051-1108 was previously solved with phases from a selenomethionyl protein derivative [3, 13]. An initial model for molecular replacement (MR) was generated from these coordinates (PDB code 1HC8) by modifying the RNA to contain the ch-like bases and removing residues 2–5 and 67–75 (containing the site of mutation, Ser69 to Asn, in L11-C76) from both copies of the protein in the asymmetric unit. Molecular replacement was performed using AMoRe [14] over the resolution range 12.0–5.0 Å with a rotational search sphere radius of 33.0 Å. The top solution had an R-factor of 36.2% and a correlation coefficient of 79.5 (both substantially better than all other solutions obtained), with no Cα-Cα close contact distances of less than 6 Å. An initial rigid-body refinement followed by subsequent rounds of restrained refinement and minimization were carried out with the CNS package [15] employing the maximum likelihood (ML) target function and bulk solvent correction. Refinement was against all reflections in the range 18–2.8 Å, with no σ cut off. The protein residues omitted during molecular replacement were built back into the model with the program O [16] guided by $2F_o - F_c$ and $F_o - F_c$ density maps generated with CNS. Over five rounds of refinement, 16 Mg^{2+} ions, two K^+ ions [13], two $Co(NH_3)_6^{3+}$ ions, eight waters, and three glycerol molecules were incorporated into the model. The final model was refined to an R_{work} of 22.7% and an R_{free} of 25.5%. Simulated annealing omit maps were generated with CNS with ch-like RNA base pair UA1062-1076 and L11 residue 69, omitted from the calculation. Data collection, processing and refinement, and model statistics are presented in Table 2.

Acknowledgments

We are grateful to the staff of beamline 9.6 at the Synchrotron Radiation Source (SRS), Daresbury Laboratories, UK, for assistance with data collection. We also thank Dr. P. Bryant for assistance with data processing, and Drs. J. Hobbs and A. Doig for helpful discussions on the manuscript. This work was supported by the CCLRC (ref. 41137), a Wellcome Trust Career Development Fellowship (ref. 061444) to G.L.C. and a BBSRC Committee Studentship to M.S.D.

Received: October 12, 2004
Revised: November 12, 2004
Accepted: November 12, 2004
Published: February 25, 2005

References

1. Mears, J.A., Cannone, J.J., Stagg, S.M., Gutell, R.R., Agrawal, R.K., and Harvey, S.C. (2002). Modeling a minimal ribosome based on comparative sequence analysis. J. Mol. Biol. *321*, 215–234.
2. Conn, G.L., Gutell, R.R., and Draper, D.E. (1998). A functional ribosomal RNA tertiary structure involves a base triple interaction. Biochemistry *37*, 11980–11988.
3. Conn, G.L., Draper, D.E., Lattman, E.E., and Gittis, A.G. (1999). Crystal structure of a conserved ribosomal protein-RNA complex. Science *284*, 1171–1174.
4. Wimberly, B.T., Guymon, R., McCutcheon, J.P., White, S.W., and Ramakrishnan, V. (1999). A detailed view of a ribosomal active site: the structure of the L11-RNA complex. Cell *97*, 491–502.
5. Sibold, C., and Subramanian, A.R. (1990). Cloning and characterization of the genes for ribosomal proteins L10 and L12 from Synechocystis sp pcc-6803—Comparison of gene clustering pattern and protein sequence homology between cyanobacteria and chloroplasts. Biochim. Biophys. Acta *1050*, 61–68.
6. GuhaThakurta, D., and Draper, D.E. (1999). Protein-RNA sequence covariation in a ribosomal protein-rRNA complex. Biochemistry *38*, 3633–3640.
7. Xing, Y.Y., GuhaThakurta, D., and Draper, D.E. (1997). The RNA

binding domain of ribosomal protein L11 is structurally similar to homeodomains. Nature Structural Biology *4*, 24–27.
8. Lu, M., and Draper, D.E. (1994). Bases defining an ammonium and magnesium ion-dependent tertiary structure within the large subunit ribosomal-RNA. J. Mol. Biol. *244*, 572–585.
9. Elrod-Erickson, M., Benson, T.E., and Pabo, C.O. (1998). High-resolution structures of variant Zif268-DNA complexes: implications for understanding zinc finger DNA recognition. Struct. Fold. Des. *6*, 451–464.
10. Misra, V.K., and Draper, D.E. (2001). A thermodynamic framework for Mg^{2+} binding to RNA. Proc. Natl. Acad. Sci. USA *98*, 12456–12461.
11. Ichetovkin, I.E., Abramochkin, G., and Shrader, T.E. (1997). Substrate recognition by the Leucyl/Phenylalanyl-tRNA-protein transferase. J. Biol. Chem. *272*, 33009–33014.
12. Draper, D.E., Bukhman, Y.V., and Gluick, T.C. (2000). Thermal methods for the analysis of RNA folding pathways. In Current Protocols in Nucleic Acid Chemistry, Volume 11.13, S.L. Beaucage, D.E. Bergstrom, G.D. Glick, and R.A. Jones, eds. (New York: John Wiley & Sons), pp. 33009–33014.
13. Conn, G.L., Gittis, A.G., Lattman, E.E., Misra, V.K., and Draper, D.E. (2002). A compact RNA tertiary structure contains a buried Backbone-K^+ complex. J. Mol. Biol. *318*, 963–973.
14. Navaza, J. (1994). AMoRe—an automated package for molecular replacement. Acta Crystallogr. A *50*, 157–163.
15. Brunger, A.T., Adams, P.D., Clore, G.M., DeLano, W.L., Gros, P., Grosse-Kunstleve, R.W., Jiang, J.S., Kuszewski, J., Nilges, M., Pannu, N.S., et al. (1998). Crystallography & NMR system: a new software suite for macromolecular structure determination. Acta Crystallogr. D Biol. Crystallogr. *54*, 905–921.
16. Jones, T.A., Zou, J.Y., Cowan, S.W., and Kjeldgaard, M. (1991). Improved methods for building protein models in electron density maps and the location of errors in these models. Acta Crystallogr. A *47*, 110–119.
17. DeLano, W.L. (2002). The PyMOL molecular graphics system (computer program). DeLano Scientific LLC, San Carlos, CA (http://www.pymol.org).

Accession Numbers

The coordinates for the ch-like rRNA-L11(C76) complex have been deposited in the RCSB PDB (code 1Y39).